Int. J. Heat Mass Transfer. Vol. 35, No. 8, pp. 2053–2056, 1992
Printed in Great Britain

0017–9310/92 $5.00 + 0.00

TECHNICAL NOTES

Dual solution for mixed convection in a horizontal tube under circumferentially non-uniform heating

D. K. CHOI and D. H. CHOI
Korea Advanced Institute of Science and Technology, Seoul, Korea

(*Received* 3 *July* 1991)

INTRODUCTION

IN THE combined free and forced laminar convection in horizontal ducts, the buoyancy force induces secondary flow, which enhances heat transfer between the wall and the fluid. There have been numerous analytical studies for various cross-sectional geometries for the uniform heat-flux or temperature boundary condition [1, 2]. Recently, Nandakumar *et al.* [3] examined the cases of circular and square ducts with the boundary conditions of axially uniform heat flux and circumferentially uniform temperature. They found the existence of a dual solution as the Dean problem in the isothermal curved tubes [4, 5], i.e. both two- and four-vortex crossflow patterns are possible in the certain region of Grashof number.

The studies for the circumferentially non-uniform boundary condition, on the other hand, are relatively few. Patankar *et al.* [6] treated the mixed convection flow in a circular tube for the axially uniform flux condition with the peripheral boundary condition of the top half insulated while the bottom half heated at a specified rate. They observed a change in the flow behavior from a two-vortex pattern to a four-vortex one as the Grashof number increases. However, they did not report a dual solution. Recently Law *et al.* [7] reexamined the problem to see whether the multiple solution is possible. They studied the mixed convection flow in square, circular and semicircular ducts with the thermal boundary conditions similar to those in Patankar *et al.* Although they found dual solutions in the square and semicircular ducts, they could obtain only the two-vortex solution for the circular duct for the entire Grashof-number region they studied ($2/\pi\, Gr < 10^5 \sim 10^6$). This finding is in contradiction to that of Patankar *et al.*, whose solution exhibits a four-vortex pattern above a certain critical Grashof number. The discrepancy of these two results has motivated us to undertake the present investigation. The purpose of this study is to clarify the matter and, if possible, to identify the regions of multiple solution for the range of Prandtl numbers.

SOLUTION PROCEDURE

For a fully developed mixed convection flow in a heated horizontal circular tube, invoking the Boussinesq approximation, the dimensionless governing equations of continuity, momentum and energy are written in the cylindrical coordinates (r, θ, z) shown in Fig. 1.

$$\frac{\partial}{\partial \eta}(\eta U) + \frac{\partial V}{\partial \theta} = 0 \tag{1}$$

$$U\frac{\partial U}{\partial \eta} + \frac{V}{\eta}\frac{\partial U}{\partial \theta} - \frac{V^2}{\eta} = -\frac{\partial P}{\partial \eta} + \nabla^2 U - \frac{2}{\eta^2}\frac{\partial V}{\partial \theta} - \frac{U}{\eta^2} + Gr\,\Phi\cos\theta \tag{2}$$

$$U\frac{\partial V}{\partial \eta} + \frac{V}{\eta}\frac{\partial V}{\partial \theta} + \frac{UV}{\eta} = -\frac{1}{\eta}\frac{\partial P}{\partial \theta} + \nabla^2 V + \frac{2}{\eta^2}\frac{\partial U}{\partial \theta} - \frac{V}{\eta^2} - Gr\,\Phi\sin\theta \tag{3}$$

$$U\frac{\partial W}{\partial \eta} + \frac{V}{\eta}\frac{\partial W}{\partial \theta} = 1 + \nabla^2 W \tag{4}$$

$$U\frac{\partial \Phi}{\partial \eta} + \frac{V}{\eta}\frac{\partial \Phi}{\partial \theta} + \frac{(W/\bar{W})}{\pi Pr} = \frac{1}{Pr}\nabla^2\Phi \tag{5}$$

where the dimensionless variables are defined as

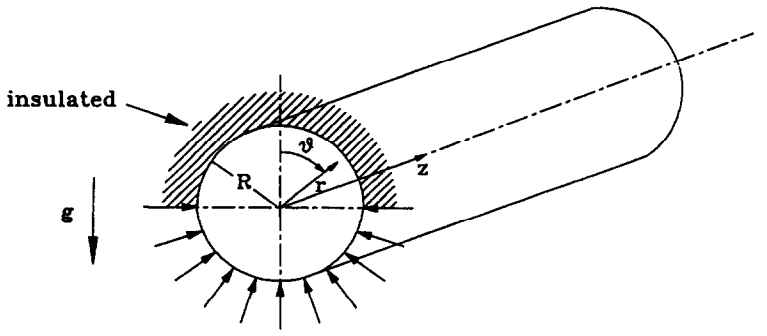

FIG. 1. Coordinate system.

NOMENCLATURE

D	tube diameter
f	friction factor, equation (10)
g	gravitational acceleration
Gr	Grashof number, equation (6)
k	thermal conductivity
Nu	average Nusselt number, equation (10)
P	dimensionless pressure, equation (6)
p	pressure
p^*	reduced pressure, equation (7)
Pr	Prandtl number, equation (6)
Q'	heat transfer rate per unit length
q	heat transfer rate per unit area
R	tube radius
r	radial coordinate
Re	Reynolds number, $\bar{w}D/\nu$
T	temperature
U, V, W	dimensionless velocities, equation (6)
u, v, w	velocity components in r, θ, z.

Greek symbols

α	thermal diffusivity
β	thermal expansion coefficient
η	dimensionless radial coordinate, r/R
θ	azimuthal coordinate
ν	kinematic viscosity
ρ	density
Φ	dimensionless temperature, equation (6)
ψ	stream function.

Subscripts

0	forced convection value
b	bulk property
w	wall value.

$$U = \frac{u}{\nu/R}, \quad V = \frac{v}{\nu/R}, \quad W = \frac{w}{(-\mathrm{d}p/\mathrm{d}z)(R^2/\rho\nu)},$$

$$\eta = \frac{r}{R}, \quad \Phi = \frac{T - T_b}{Q'/k}, \quad P = \frac{p^*}{\rho(\nu/R)^2},$$

$$Gr = Q'g\beta R^3/k\nu^2, \quad Pr = \nu/\alpha \tag{6}$$

and

$$p^* = p + \rho_b g r \cos\theta. \tag{7}$$

Here, (u, v, w) are the velocity components in the (r, θ, z) directions and the overbar denotes the average value. Since the flow is symmetric, it suffices to consider only half the tube cross section $(0 \leqslant \theta \leqslant \pi)$. The boundary conditions may then be expressed as

$\eta = 1$: $U = V = W = 0$ (no-slip)

$\eta = 1, 0 \leqslant \theta \leqslant \frac{\pi}{2}$: $\frac{\partial \Phi}{\partial \eta} = 0$ (adiabatic)

$\eta = 1, \frac{\pi}{2} \leqslant \theta \leqslant \pi$: $\frac{\partial \Phi}{\partial \eta} = \frac{1}{\pi}$ (uniform heat flux)

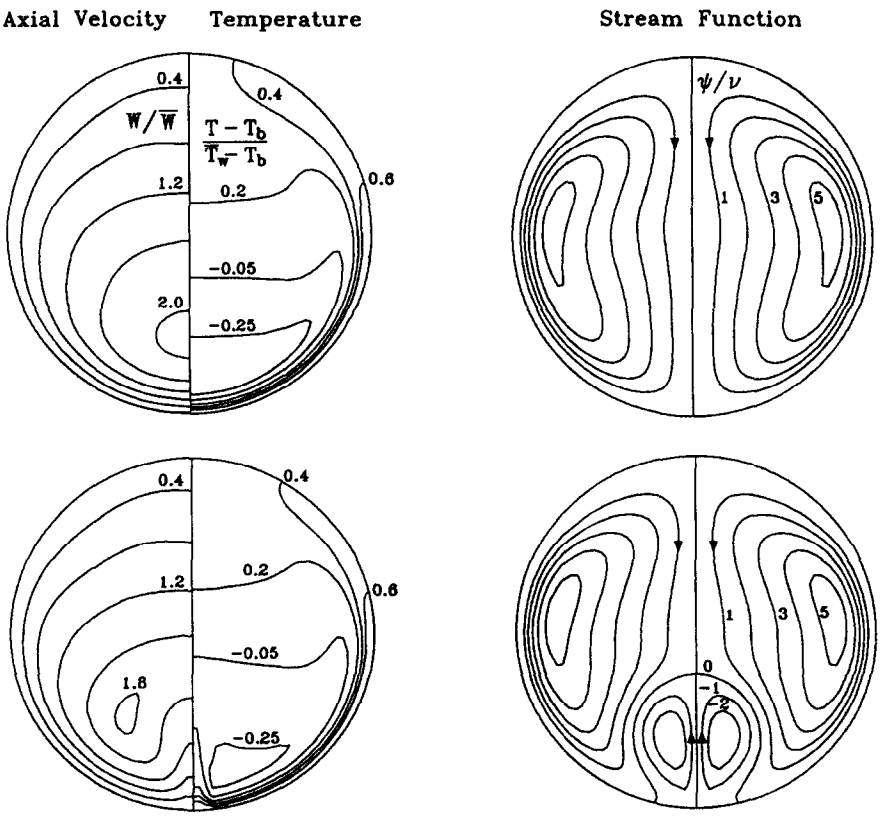

FIG. 2. Contours of axial velocity, temperature, and stream function for $Pr = 5$, $2/\pi\, Gr = 10^6$.

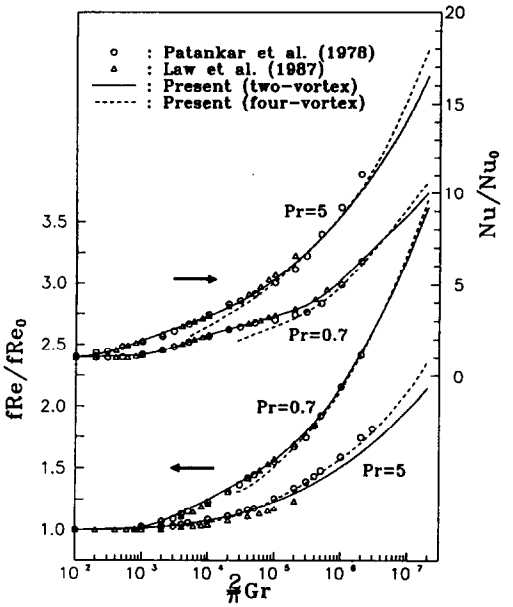

FIG. 3. Friction factor and Nusselt number variation with Grashof number.

$$\theta = 0, \theta = \pi: \quad V = 0, \quad \frac{\partial U}{\partial \theta} = \frac{\partial W}{\partial \theta} = \frac{\partial \Phi}{\partial \theta} = 0 \quad \text{(symmetry)}. \tag{8}$$

In addition, the introduction of the bulk temperature requires the solution to satisfy the overall energy balance, which is

$$\int_0^1 \int_0^{\pi} \Phi W \eta \, d\eta \, d\theta = 0. \tag{9}$$

These equations are discretized on a staggered grid: the QUICK scheme of Leonard [8] is adopted for the convective derivatives to reduce the error due to numerical diffusion, whereas the central differencing is used for other derivatives. Using the SIMPLER algorithm of Patankar [9], the solution is sought iteratively until the following convergence criteria are met:

$$\Sigma(|\mathrm{Res}_Q|) < 5 \times 10^{-4} \quad (Q: \text{continuity}, U, V, W, \Phi \text{ equations})$$

and

$$|Q^{n+1} - Q^n|/|Q^n| < 10^{-5} \quad (Q: f\,Re \text{ and } Nu).$$

RESULTS AND DISCUSSION

The calculations have been performed first for two Prandtl numbers, i.e. 0.7 and 5, and $2/\pi\,Gr$ ranging from 10^2 to 10^8 for each Prandtl number as done in refs. [4, 5]. In order to insure that the grid is sufficiently fine, a few different grids were tested for $Pr = 5$ at $2/\pi\,Gr = 10^7$. A 40×40 grid, which is uniform in the circumferential direction and densely distributed near the wall in the radial direction, was found adequate and used throughout in the present study. Incidentally, this particular grid distribution is much finer than the ones used in the previous studies [6, 7].

For the case of $Pr = 5$, the present results exhibit the existence of two solutions when $2/\pi\,Gr > 5.3 \times 10^3$: the cross-flow pattern of either two-vortex or four-vortex type is found possible. If the solution is obtained in the direction of increasing Gr using the flow field of a lower Gr as an initial guess, the resulting flow pattern is of two-vortex type whereas the four-vortex solution results if the four-vortex solution of a higher Gr is used as an initial guess. This means that, for a certain range of Gr, either type of flow field is possible as is shown clearly in Fig. 2. The phenomenon was not identified in the earlier studies: although both types of solution were reported by Patankar *et al.* [6], each occurs in a different Gr region, whereas no four-vortex solution could be obtained by Law *et al.* [7].

The friction coefficient and the averaged Nusselt number are plotted in Fig. 3. The increasing values indicate that the secondary motion of the flow becomes more active as Gr increases; the figure shows that the results for corresponding flow types are in close agreement with the earlier results. Here, the friction factor f and the Nusselt number are defined as

$$f = \frac{(-dp/dz)D}{\frac{1}{2}\rho \bar{w}^2}, \quad Nu = \frac{qD}{k(\bar{T}_w - T_b)} \tag{10}$$

with

$$\bar{T}_w = \frac{1}{\pi} \int_{\pi/2}^{3\pi/2} T_w \, d\theta.$$

The region of dual solution begins at $2/\pi\,Gr = 5.3 \times 10^3$. This critical point remained fixed as we tried different grids and thus introduced varying degrees of disturbance in the calculation. On the other hand, the upper limit of Gr could not be placed definitely. With the present 40×40 non-uniform grid, the two-vortex solution can be maintained throughout the region of investigation ($2/\pi\,Gr \leqslant 10^8$). However, when the 30×30 uniform grid was used earlier in the study, the solution changed from two-vortex type to that of four-vortex at $2/\pi\,Gr \approx 2 \times 10^7$. This suggests that the 30×30 uniform grid is not sufficient to locate such a point. Based on the present results, the upper limit of $2/\pi\,Gr$ is greater than 10^8 and can be confirmed only when the solutions of two different grids coincide.

Now we turn the attention to the flow for $Pr = 0.7$. Here, initially, the two-vortex flow pattern persisted for the entire Grashof-number range: unlike in the case for $Pr = 5$, the flow did not change naturally to that of four-vortex type. This appeared to be in accordance with the results by Law *et al.* [7], but different from that of Patankar *et al.* [6] in which a spontaneous four-vortex pattern was reported for the large Gr region. It is not the whole picture though: a four-vortex solution was found later when we tried to locate the bifurcation point for other Prandtl-number flows. Using the four-vortex solution of $Pr = 5$ as an initial guess, the solution, which is of four-vortex type, for a neighboring Pr was obtained. In this manner, the four-vortex solution could be maintained for Pr as small as 0.2. Both solutions for $Pr = 0.7$ and $2/\pi\,Gr = 10^6$ are depicted in Fig. 4. It is observed from the figure that, due to the thicker thermal layer, the secondary motion of the flow is much more pronounced here than in the case for $Pr = 5$. Figure 3 presents the friction coefficient and the average Nusselt number. Here again, the results are seen to be in good agreement with the previous results when the flow patterns are matched.

Finally the Pr–Gr relation that demarcates the two solution regions is given in Fig. 5: as Pr increases, critical Gr decreases rather sharply initially and more moderately later on. It also shows that the dual solution exists throughout the Pr range that has been examined ($0.2 \leqslant Pr \leqslant 10$).

The present paper has illuminated the duality of the solution in the fully developed region. How the flow reaches to those two different final states is largely in question. To shed some light on the subject, the entrance region of the tube is currently examined by the authors.

SUMMARY

The fully developed mixed convection flow in a circular pipe, the top half of which is insulated and the bottom half is maintained at the constant heat-flux condition, has been numerically investigated. The dual solution, which was not identified in the earlier studies, has been observed for the

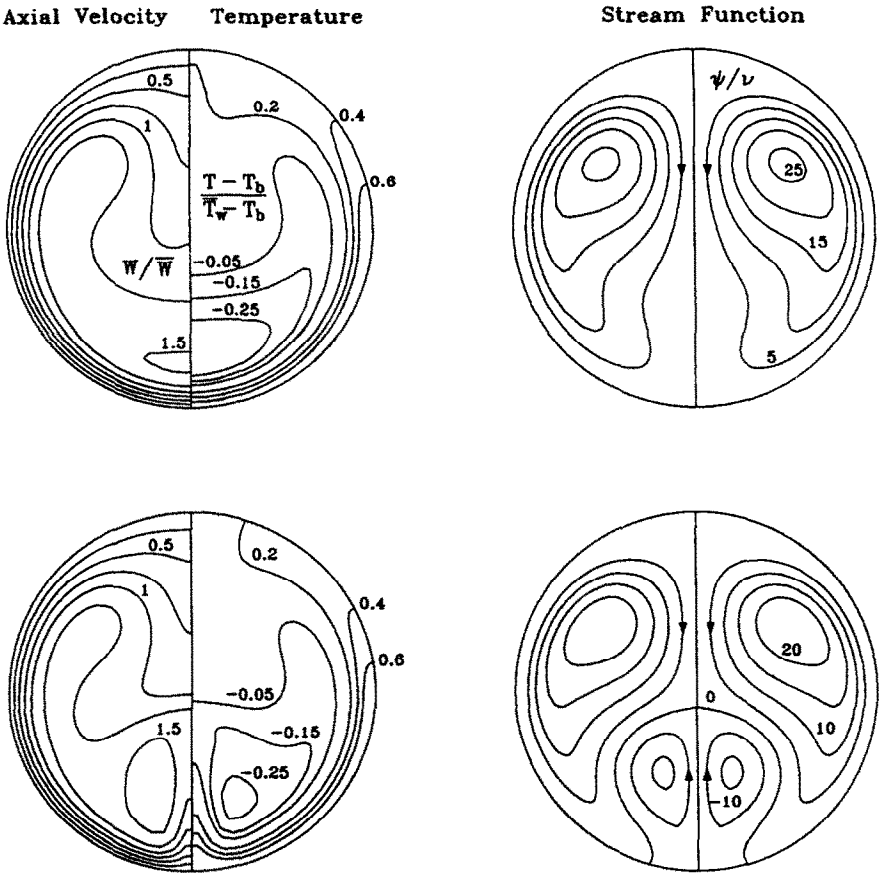

FIG. 4. Contours of axial velocity, temperature, and stream function for $Pr = 0.7$, $2/\pi\, Gr = 10^6$.

range of Prandtl number ($0.2 \leqslant Pr \leqslant 10$). The lower end of the dual-solution region, Gr_{crit}, has been located. The upper limit of Gr, on the other hand, appears to be more susceptible to disturbances and is dependent upon the grid being used. The dual solution could be maintained up to $2/\pi\, Gr \leqslant 10^8$ for $Pr = 5$, which is the highest Gr examined in the study.

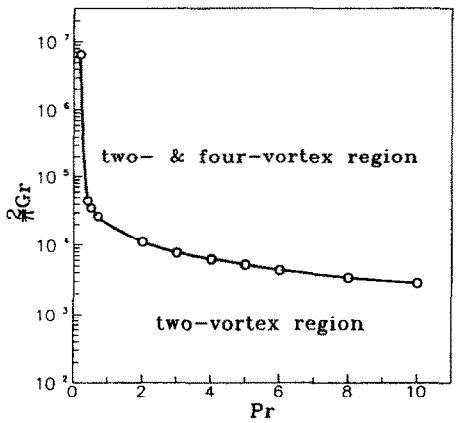

FIG. 5. Bifurcation map.

REFERENCES

1. P. H. Newell and A. E. Bergles, Analysis of laminar combined free and forced convection for fully developed laminar flow in horizontal tubes, *J. Heat Transfer* **92,** 83–93 (1970).
2. F. C. Chou and G. J. Hwang, Combined free and forced laminar convection in horizontal rectangular channels for high *Re Ra*, *Can. J. Chem. Engng* **62,** 830–836 (1984).
3. K. Nandakumar, J. H. Masliyah and H. S. Law, Bifurcation in steady laminar mixed convection flow in horizontal ducts, *J. Fluid Mech.* **152,** 145–161 (1985).
4. J. H. Masliyah, On laminar flow in curved semi-circular ducts, *J. Fluid Mech.* **99,** 469–479 (1980).
5. K. Nandakumar and J. H. Masliyah, Bifurcation in steady laminar flow through curved tubes, *J. Fluid Mech.* **119,** 475–490 (1982).
6. S. V. Patankar, S. Ramadhyani and E. M. Sparrow, Effect of circumferencially nonuniform heating on laminar combined convection in a horizontal tube, *J. Heat Transfer* **100,** 63–70 (1978).
7. H. S. Law, J. H. Masliyah and K. Nandakumar, Effect of nonuniform heating on laminar mixed convection in ducts, *J. Heat Transfer* **109,** 131–137 (1987).
8. B. P. Leonard, A stable and accurate convective modelling procedure based on quadratic upstream interpolation, *Comput. Methods Appl. Mech. Engng* **19,** 59–98 (1979).
9. S. V. Patankar, *Numerical Heat Transfer and Fluid Flow*, McGraw-Hill, New York (1980).